Solvothermal modified nano-titania as the potential photocatalyst for the degradation of organic dyes

T Kishore Kumar [a], Prasanna [a], P Ajith [b], D Prem Anand [*b]

[a] Talent Development Centre, Indian Institute of Science Challakere Campus at Khudapura, Chitradurga, Karnataka 577536, India.

[b] Department of Physics, St.Xavier's College (Autonomous), Palayamkottai 627002 Tamil Nadu, India.

Abstract

High yield nano-titania was synthesized by a one-step solvothermal process. The catalyst was characterized by XRD, FTIR, UV-VIS-NIR, and SEM analysis. The phase structure and morphology of the as-prepared nano-titania were confirmed by XRD and SEM analysis. The FTIR and optical absorption studies confirmed the structure of nano-titania. Scanning electron microscopic observations revealed that the morphology of nano-titania with anatase structure. The photocatalytic activity of the catalyst is explored in the degradation of methylene blue dye. The present catalyst shows effective degradation of methylene blue under solar radiation. An attempt for the bulk degradation of methylene blue dye is also carried out.

Graphical Abstract

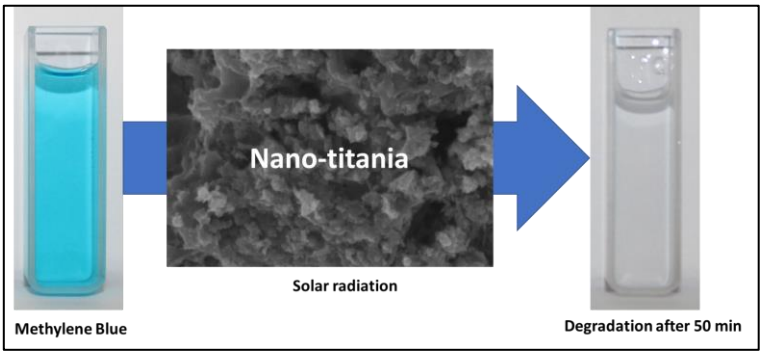

Keywords: Nano-titania, Solvothermal synthesis, Photocatalytic activity, Anatase TiO_2.

Introduction

Rising environmental issues like water pollution by industrial wastes mainly organic dyes should be treated before it reaches water sources.[1-3] Because it will pollute the freshwater sources and there is a lack of freshwater sources in the world.[4-5] In water treatment, photocatalysts can be employed efficiently to complete the mineralization of organic pollutants.[6-9] Although zinc oxide and cadmium sulfides are used in photocatalysis, titanium dioxide is quite good among all photocatalysts.[10-11] In general, anatase TiO_2 is more active in photocatalytic degradation than rutile TiO_2 because of the thermodynamic stability of the rutile phase.[12-15] One-dimensional nanostructured materials including nanotubes, nanorods, and nanowires have attracted considerable attention because of their unique electronic and optical properties and their potential applications in modern technology. It has been found that the properties of these nanoparticles strongly depend on their size and shape. Hence it is crucial to control their size and the overall morphology to make use of them in suitable applications.[16-18] TiO_2 is an n-type semiconductor that is chemically stable as well as stable towards photo-oxidation. It is non-toxic and relatively easy and cheap to produce. Therefore, it has been functional in many applications such as solar cells, gas sensors, electrochemical capacitors, rechargeable lithium batteries, catalysis, and photocatalysis, etc.[19-24]

TiO_2 nanotubes have been synthesized by various techniques such as chemical vapor deposition, thermal evaporation, and hydrothermal method.[25] The first hydrothermal route was discovered by Kasuga for the synthesis of titanate nanotubes.[19-20] Weng et al suggested increasing the hydrothermal duration the length of the nanotubes increases if the treatment duration exceeded 24 hours.[26] Yuan and coworkers also reported that the formation of TiO_2 nanotubes and nanoribbons are affected only by the treatment temperature.[27-28] In this study, nano-titania was prepared via a solvothermal process in a 10 M NaOH solution at 170^{o} C for

12 hours followed by washing with HCl solution and distilled water. The as-prepared nano-titania were characterized by XRD, FTIR, UV–Vis-NIR, and SEM analysis. The photocatalytic activity of the nano-titania is explored in the degradation of methylene blue (MB) dye. An approach for effective bulk degradation of MB dye is also discussed.

2. Experimental

2.1 Sample preparation

The nano-titania was prepared using a chemical process explained below. Exactly 1g of commercial TiO_2 nanopowder was added to 100 mL of 10 M NaOH solution. The mixture was stirred for 30 minutes in a beaker. It was then transferred into a Teflon-lined stainless steel autoclave of 100 ml capacity till about 90% of the total volume, heated at 170^0 C up to 12 hours. The autoclave was cooled to room temperature, and the sample was filtered and washed with distilled water. After that, acid washing was done with 0.1 N HCl for 6 hours. Then it was washed several times with water till the pH value reached 7 and the sample was dried at 80^0 C for 9 hours.

2.2 Characterizations

The crystal structure and morphology of the as-prepared nano-titania were characterized by XRD, FTIR, UV-VIS-NIR, and SEM analysis. The PXRD was carried out using a PANalytical Empyrean powder XRD diffractometer with Cu Kα as the source. FTIR analysis was carried out in the Perkin Elmer Infrared L 1600300 Spectrum Two LI Ta instrument in the range of 4000 – 400 cm^{-1}. The optical reflectance spectrum of the product was done in a Shimadzu UV – 1800 double-beam spectrometer supported by Shimadzu UV probe software, and version 2.52 was used. The SEM images were taken with a scanning electron microscope EVO 18, Germany Carl Zeiss Corporation.

2.3 Photocatalytic activity

The photocatalytic activity of the nano-titania is studied in a photocatalytic reactor with a 1000 W halogen lamp as a light source. The distance between the source and the reactor is 0.65 m. All the experiments are carried out at room temperature and the temperature is maintained by an air-cooled system. 50 mL of the known concentration of MB dye is taken each time for degradation. 2 mL of the dye solution is taken out and centrifuged each time to monitor the degradation. The UV-Visible absorption spectrum of the solution is recorded in the range of 450 – 750 nm up to 1.5 hours. The photocatalytic degradation of MB dye in sunlight was carried out in a borosil reactor with a volume of 250 mL.

3. Result and Discussions

3.1 Structure of the catalyst

XRD analysis

The XRD pattern of nano-titania is shown in Fig.1. The XRD peaks at 25.3°, 37.0°, 37.9°, 38.6°, 48.1°, 54.0°, 55.0°, 62.8°, 68.9°, 70.5°, 75.3° can be attributed to 101, 103, 004, 112, 200, 105, 211, 204, 116, 220, and 215 planes respectively in the crystalline structure of anatase synthesized nano-titania [anatase XRD JCPDS no: 18-2486]. The diffractogram also indicates that the nano-titania are well-crystallized anatase titania with a minor sodium titanate phase.[29] The crystallite size can be determined by the Scherrer formula $D = k\lambda / \beta \cos \theta$. Here λ is the wavelength of the X-ray radiation Cu Kα = 0.1540 nm. k is a constant taken as 0.89, β is the line width at half maximum height (FWHM) of the peak and θ is the diffracting angle the (101) plane was used to calculate the crystallite size. The average crystallite size of the nano-titania was found to be 47 nm.

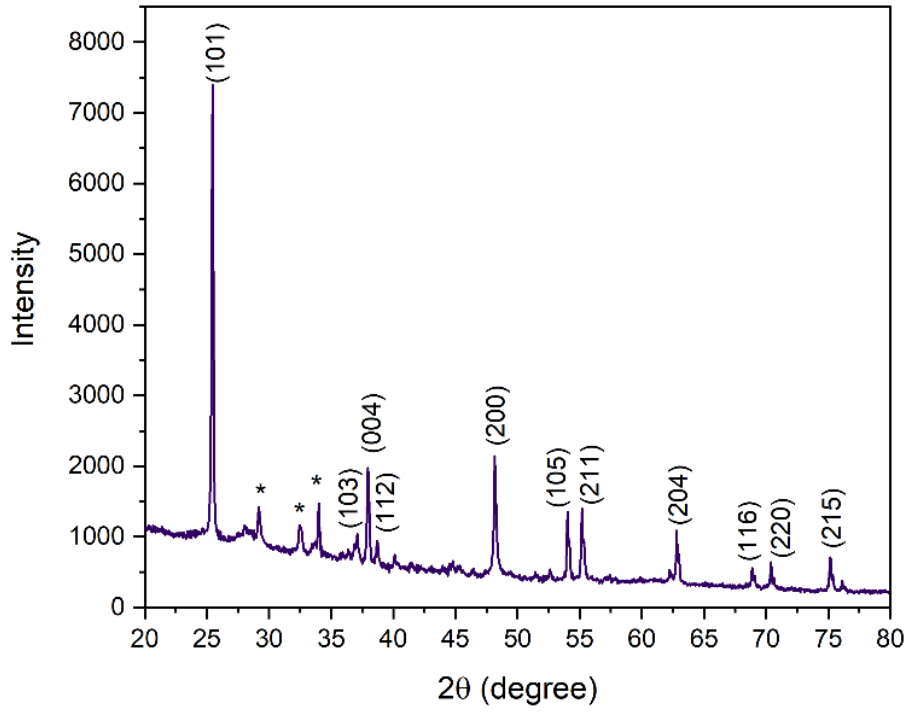

Fig 1. X-Ray Diffraction spectrum of nano-titania (* sodium titanate phase).

FTIR analysis

The FTIR spectrum of nano-titania is given in Fig.2. A broad band at 3358 cm^{-1} is observed corresponding to the O-H stretching vibration of adsorbed H_2O molecules and surface hydroxyl groups. Some weak vibrational bands appear near 2350 cm^{-1} are due to adsorbed CO_2 molecules. The presence of the band at 1642 cm^{-1} is due to the bending vibrational mode of adsorbed water.[30] The absorption band at 1455 cm^{-1} is due to the presence of some OH groups on the surface of titanate nanocrystals. Another broad band appearing at 450 cm^{-1} which is attributed to TiO_2.[31]

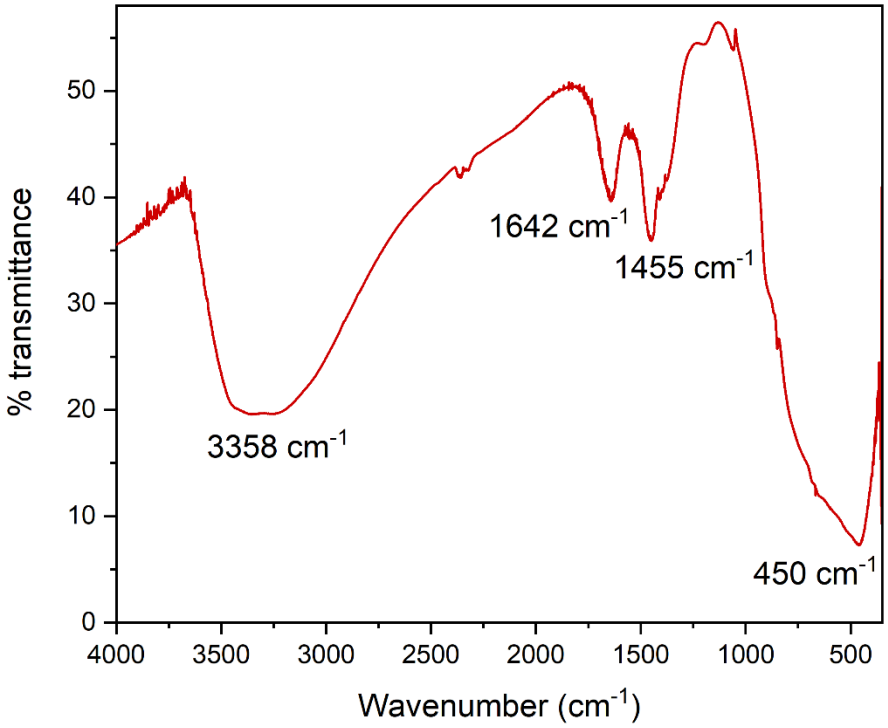

Fig.2: FTIR spectrum of nano-titania.

UV-VIS- NIR analysis

The optical absorption spectrum of nano-titania in the range of 190 nm – 1100 nm is shown in Fig.3. The absorption study revealed that the nano-titania is transparent in the visible region. The absorption peak is starting from 447 nm is identified by drawing a tangent to X-axis and the absorption maximum is observed at 259 nm. Hence the bandgap energy of nano-titania is 2.77 eV which is comparable with the bandgap of the anatase titania.[32]

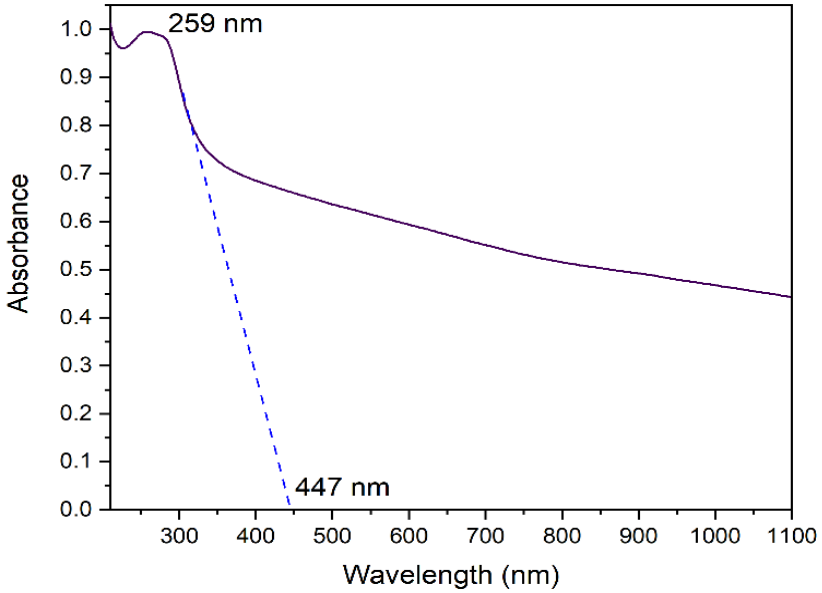

Fig 3. The absorption spectrum of nano-titania.

SEM analysis

The SEM micrographs of nano-titania are given in Fig.4. It is observed that the micrographs exposed cluster appearances with crystalline nature. However spherical structures with irregular surfaces morphologies are seen in Fig.4a. There is an increased grain size due to the increase in temperature leading to crystalline as well as grain growth. The strong appearance might have been due to the aggregation of nano-titania ranging between 100 – 150 nm in size (Fig.4b).

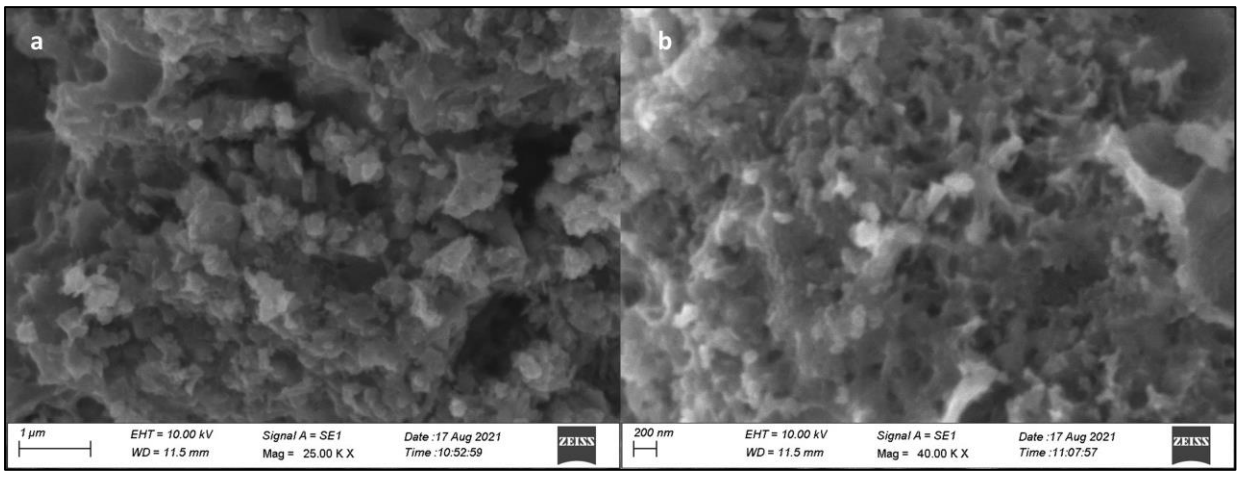

Fig.4: SEM image at (a)1 μm and (b) 200 nm of nano-titania.

3.2 Photocatalytic activity of the catalyst

The photocatalytic activity of the catalyst is studied in the presence of a halogen lamp as well as solar radiation. The optimization and comparison studies are carried out in a photocatalytic reactor with a halogen lamp as a light source. The emission spectra of the solar radiation and halogen lamp is given in Fig.5. The halogen lamp consists of almost all the wavelengths similar to the solar radiation and the emission starts from 300 nm in both spectra. But the intensity corresponding to the UV region is more in the solar spectrum than in the case of the halogen lamp. So, we employed a halogen lamp in the optimization studies.

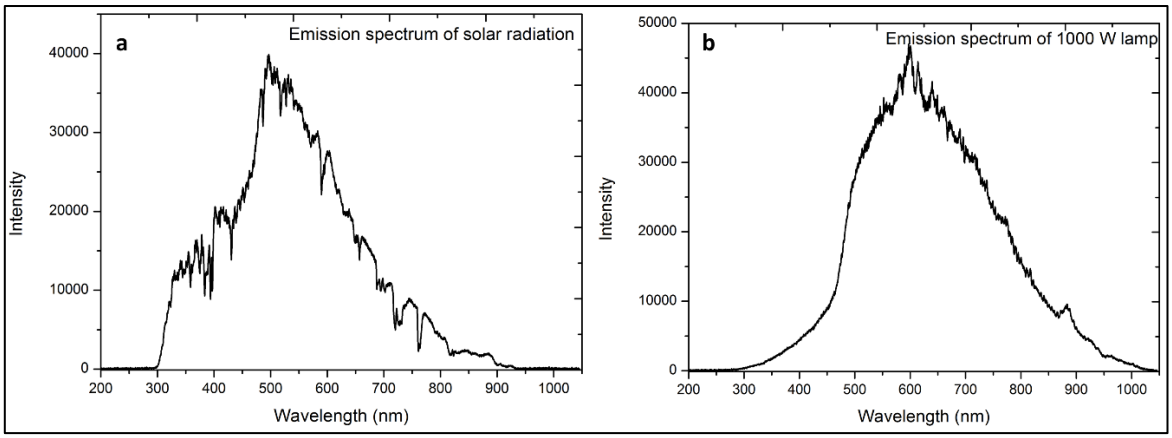

Fig.5: Emission spectra of (a) solar radiation and (b) halogen lamp.

Effect of catalyst loading

The effect of catalyst loading in the degradation of methylene blue dye is evaluated by varying the amount of the catalyst from 0.00 kg/m^3 to 1.00 kg/m^3 given in Fig.6a. The initial concentration of the dye is 1.56×10^{-5} moldm^{-3} that is kept constant. The degradation of the dye is monitored by recording the UV-visible spectrum in regular intervals up to 1.5 h.

Without the catalyst, there is no degradation was observed. The degradation is increased with an increase in the catalyst loading up to 0.1 kgm^{-3}. After that, the degradation of methylene blue dye is decreased. The degradation percentage in all the cases is calculated using the formula, $\%\ \text{degradation} = \left(1 - \frac{A}{A_o}\right) \times 100$, where A is the absorbance at 1.5 h, and A_o is the initial absorbance. The degradation percentage in the case of 0.1 kgm^{-3} of catalyst loading is maximum and that is 78.6 %.

The optimization of catalyst loading in MB dye degradation is determined from another parameter also. The degradation of the dye at lower concentrations follows quasi-first-order kinetics. So, the apparent rate constant is calculated by plotting $\ln(A/A_o)$ versus time. The apparent rate constant in each case is plotted versus catalyst loading given in Fig.6b. The rate constant increases up to 0.1 kgm^{-3} (14.12×10^{-3} min^{-1}) and then it decreases. Therefore, the catalyst loading of 0.1 kgm^{-3} is considered as optimum catalyst loading for the degradation of MB dye.

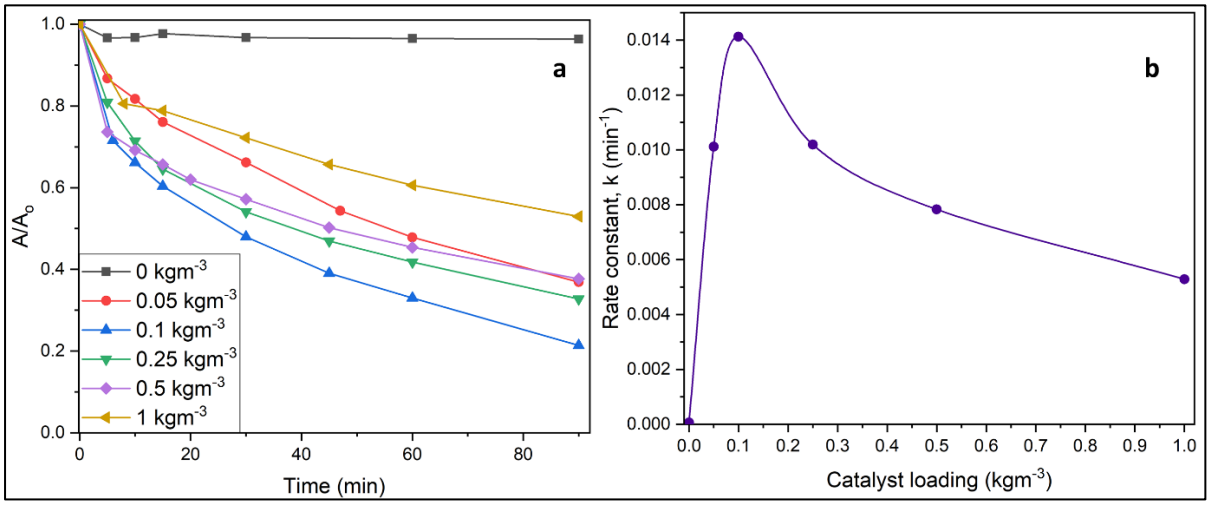

Fig.6: (a) Degradation profile of methylene blue and (b) plot of apparent rate constant.

Effect of initial concentration

The effect of the initial concentration of the methylene blue dye is studied by decreasing the concentration given in Fig.7. There is no big breakthrough in the degradation percentage by varying the concentration. But in the case of initial concentration of 0.938×10^{-5} mol/L, the apparent rate constant value is high and that is 16.58×10^{-3} min^{-1}. So, the initial concentration of 0.938×10^{-5} mol/L is considered to be the optimum condition. Therefore, the methylene blue dye with an initial concentration of 0.938×10^{-5} mol/L and 0.1 kgm^{-3} of catalyst loading are chosen as a standard condition for dye degradation.

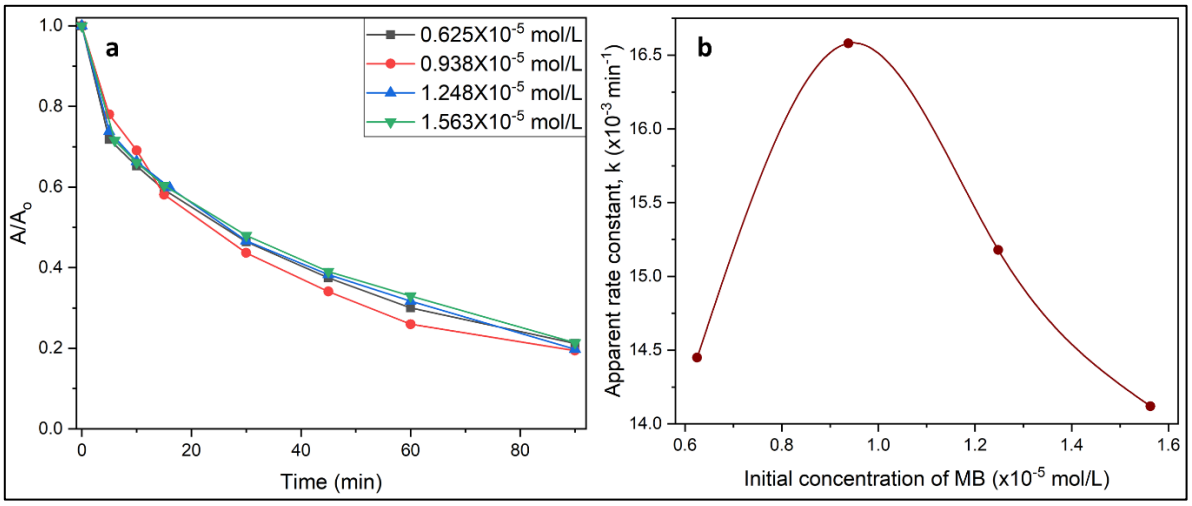

Fig.7: (a) degradation profile and (b) plot of apparent rate constant for various initial concentrations of the dye.

Comparison with the precursor

The photocatalytic activity of the present catalyst is compared with commercial TiO_2 which is used as the precursor in the synthesis of the catalyst. The catalyst comparison is carried out in the optimized reaction condition in the degradation of MB dye given in Fig.8. The photocatalytic activity of commercial TiO_2 is very less compared to nano-titania in optimized reaction conditions. The apparent rate constant of the degradation in the presence of nano-titania is 8 times more than commercial TiO_2 catalyst. So, the solvothermal synthesized nano-

titania are efficient and highly suitable for the degradation of methylene blue. Moreover, commercial TiO_2 disperse in the dye solution forms the colloidal solution. So, the separation of the catalyst from the degraded dye solution becomes a very tedious process. But, the solvothermal synthesized nano-titania are fully heterogeneous in the solution. Therefore we can separate by centrifugation with ease.

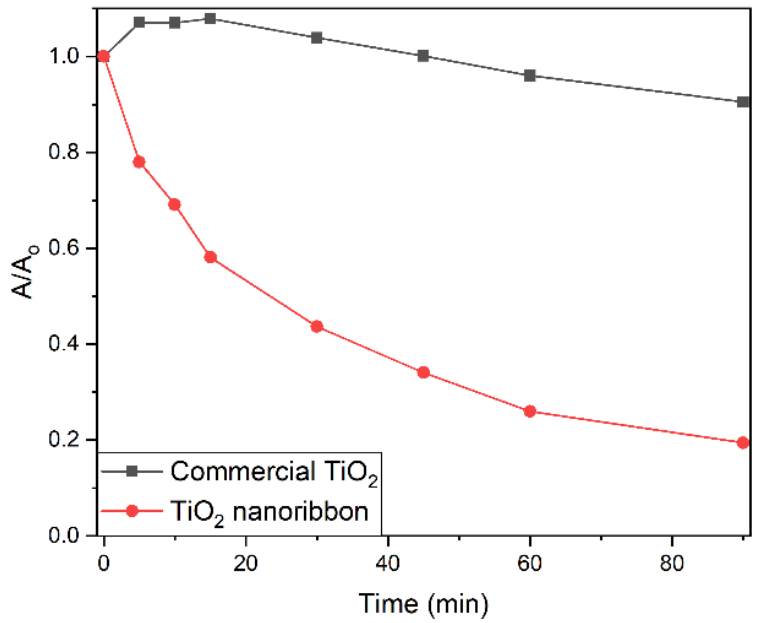

Fig.8: Degradation profile of commercial TiO_2 and nano-titania.

Degradation of methylene blue under solar radiation

The degradation of the MB dye under solar radiation is carried out in the optimized reaction condition (Fig.9). Our delightful, the degradation in presence of solar radiation is much faster than in the case of the halogen lamp. In 50 minutes, 92.04% of methylene blue dye degraded is shown in Fig.9. The apparent rate constant value is 47.1×10^{-3} min^{-1} which is 2.8 times more than that in presence of a halogen lamp. This is because of the more intensity of radiation in the UV region in the case of solar radiation.

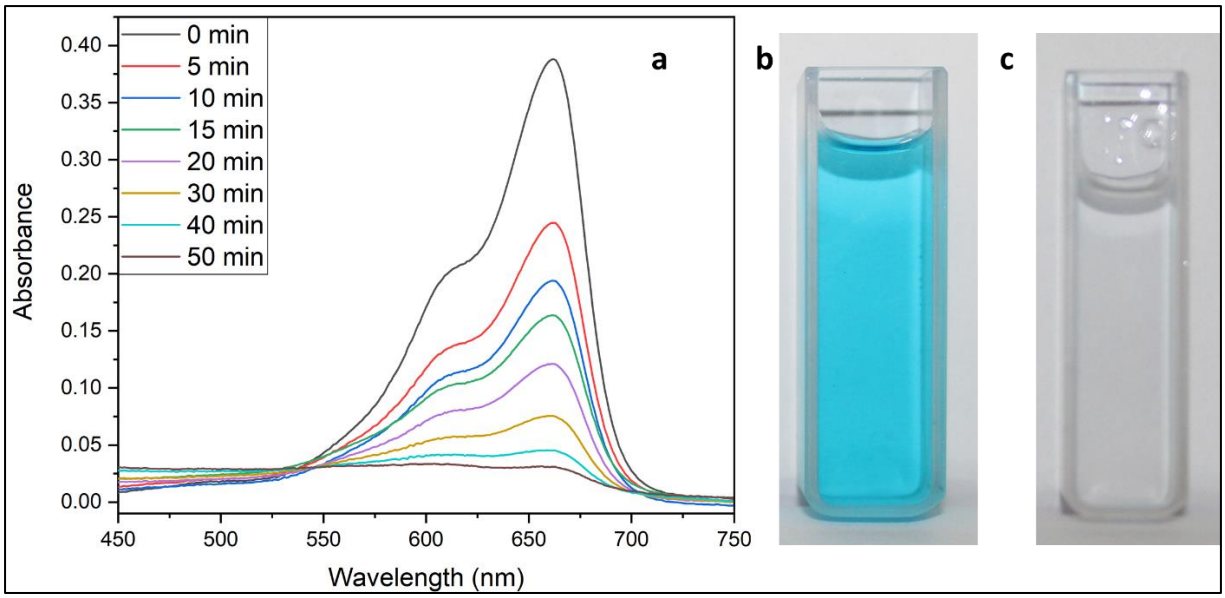

Fig.9: (a) degradation profile of MB in presence of solar radiation, photographs of the dye (b) before and (c) after the degradation.

It is important to study the photocatalytic activity of the catalyst on a large scale, mainly in the industries. So, we extended our study to the bulk degradation of 1 L methylene blue dye under sunlight. From the optimization studies, the catalyst required for the degradation of 1 L MB dye is 100 mg. This study is carried out in a 1 L borosil reactor with a glass window. We got 90.1% degradation of MB dye in 1.25 h with an apparent rate constant of 33.41×10^{-3} min^{-1}. The relative decrease in the rate of degradation is because of a lesser area of exposure to sunlight. Therefore, we can degrade the bulk amount of MB dye in presence of nano-titania with ease.

A plausible mechanism for photocatalytic activity of nano-titania

The mechanism of dye degradation is depending on the electron-hole pair formed in the catalyst.[32] Solar radiation irradiation resulting the transition of an electron to the conduction band and leaving a hole in the valence band as follow: $TiO_2 + h\nu \rightarrow h^+_{VB} + e^-_{CB}$. Trapping of

H_2O as well as OH^- by the hole form $OH^\cdot$ radicals: $h_{VB}^+ + H_2O \rightarrow H^+ + OH^\cdot$ and $h_{VB}^+ + 2OH^- \rightarrow OH^- + OH^\cdot$. Electrons are trapped by the molecular oxygen-producing superoxide ion and further form $OH^\cdot$ radicals: $e_{CB}^- + O_2 \rightarrow O_2^{\cdot-} \Rightarrow H_2O + O_2^{\cdot-} \rightarrow OH^- + OH^\cdot + \frac{1}{2}O_2$. The hydroxyl radicals obtained in these reactions will oxidize the dye molecules in the solution. Therefore, the degradation of dye molecules in the solution takes place with the decolorization of the dye solution.

Catalyst comparison

The photocatalytic activity of nano-titania is compared with reported catalysts given in Table 1. Clearly, the present catalyst shows very good photocatalytic activity with less amount catalyst loading and the catalyst preparation protocol is also easier.

Table 1: Comparison of photodegradation of MB dye by using different photocatalysts.

Catalyst	Method of preparation	Light irradiated	Time (min)	Catalyst loading (g/L)	% degradation
$AgTi_5$	Sol-gel	UV	200	1.0	97.1[33]
TiO_2-curcumin	Sol-gel	UV	90	1.0	91.0[34]
Cu-TiO_2/ZnO	Sol-gel	Visible light	120	1.5	73.5[35]
0.5%Pd-TiO_2	Sol-gel	UV	120	1.0	99.4[36]
Nano-titania	Solvothermal	Sunlight	50	0.1	92.04 (This work)

4 Conclusions

In summary, a modified nano-titania-based catalyst was synthesized by the one-step solvothermal method. From the PXRD, the anatase TiO_2 is a major phase and the average crystallite size of the nano-titania was estimated to be 47 nm. From the FTIR and UV-Vis-NIR spectral analysis, the structure of the catalyst is confirmed. The SEM micrographs clearly reveal the formation of nano-titania with its morphology. The photocatalytic activity of the catalyst is explored in the degradation of methylene blue dye. The bulk degradation of the MB dye is also studied. The catalyst showed enhanced activity under solar radiation in the degradation of methylene blue dye.

5 Reference

1. B. Lai, Subhash C. Singh, J.K. Bindrab, C.S. Saraj, A. Shukla, T.P. Yadav, W. Wu, S.A. McGill, N.S. Dalal, Amit Srivastava, Chunlei Guoac Hydrogen evolution reaction from bare and surface-functionalized few-layered MoS_2 nanosheets in acidic and alkaline electrolytes, Mater. Today Chem., 14 (2019), p. 100207
2. M. Nie, H. Sun, J. Liao, Q. Li, Z. Xue, F. Xue, F. Liu, M. Wu, T. Gao, L. Teng, Study on the catalytic performance of Pd/TiO_2 electrocatalyst for hydrogen evolution reaction, Int. J. Hydrog. Energy, 46 (2021), pp. 6441-6447
3. H. Li, H. Shen, L. Duan, R. Liu, Q. Li, Q. Zhang, X. Zhao, Enhanced photocatalytic activity and synthesis of ZnO nanorods/MoS_2 composites Superlattices, Microstruct., 117 (2018), pp. 336-341
4. K. Ravichandran, E. Sindhuja, Fabrication of cost effective g-C_3N_4+Ag activated ZnO photocatalyst in thin film form for enhanced visible light responsive dye degradation, Mater. Chem. Phys., 221 (2019), pp. 203-215
5. R. Kumar, J. Rashid, M.A. Barakat, Zero valent Ag deposited TiO_2 for the efficient photocatalysis of methylene blue under UV-C light irradiation, Colloids Interface Sci. Commun., 5 (2015), pp. 1-4,

6. R. Xu, Photocatalysis, Beilstein J. Nanotechnol., 5 (2014), pp. 1071-1072
7. James F.Tanguay, Steven L. Suib, Robert W. Coughlin, Dichloromethane photodegradation using titanium catalysts, J Catal., 117 (1989), pp. 335-347
8. Ralph W. Matthews, Photocatalytic oxidation of chlorobenzene in aqueous suspensions of titanium dioxide, J Catal., 97 (1986), pp. 565-568
9. J. Chen, L. Eberlein, Cooper H. Langford, Pathways of phenol and benzene photooxidation using TiO2 supported on a zeolite, J. Photochem. Photobiol. A., 148 **(**2002**),** pp. 183-189
10. D.F. Ollis, Solar-Assisted Photocatalysis for Water Purification: Issues, Data, Questions. In: E. Pelizzetti, M. Schiavello, (Eds.), Photochemical Conversion and Storage of Solar Energy, Kluwer Academic Publishers, 1991, pp. 593-622
11. J. Augustynski, The role of the surface intermediates in the photoelectrochemical behaviour of anatase and rutile TiO_2, Electrochim. Acta, 38 (1993), pp. 43-46
12. H. Harada, T. Ueda, Photocatalytic activity of ultra-fine rutile in methanol-water solution and dependence of activity on particle size, Chem. Phys. Lett., 106 (1984), pp. 229-331
13. S.I. Nishimoto, B. Ohtani, H. Kajiwara and T. Kagiya, Correlation of the crystal structure of titanium dioxide prepared from titanium tetra-2-propoxide with the photocatalytic activity for redox reactions in aqueous propan-2-ol and silver salt solutions, J. Chem. Soc., Faraday Trans. 1, 81 (1985), pp. 61-68
14. R.I. Bickley, T.G. Carreno, J.S. Lees, L. Palmisano, R.J.D Tilley, A structural investigation of titanium dioxide photocatalysts, J. Solid State Chem., 92 (1991), pp. 178-190
15. D.R. Lide, Handbook of Chemistry and Physics, 84th ed., CRC Press, 2004.
16. A.M. Morales, C.M. Lieber, A Laser Ablation Method for the Synthesis of Crystalline Semiconductor Nanowires, Science, 279 (1998), pp. 208-211

17. J.J. Shiang, A.V. Kadavanich, R.K.Grubbs, A.P. Alivisatos, Symmetry of Annealed Wurtzite CdSe Nanocrystals: Assignment to the C3v Point Group, J. Phys. Chem., 99 (1995), pp. 17417-17422
18. T.S. Ahmadi, Z.L. Wang, T.C. Green, A. Henglei, M.A. El-sayed, Shape-Controlled Synthesis of Colloidal Platinum Nanoparticles, Science, 272 (1996), pp. 1924-1925
19. T. Kasuga, M. Hiramatsu, A. Hoson, T. Sekino, K. Niihara, Formation of Titanium Oxide Nanotube, Langmuir, 14 (1998), pp. 3160-3163
20. T. Kasuga, M. Hiramatsu, A. Hoson, T. Sekino, K. Niihara, Titania nanotubes prepared by chemical processing, Adv. Mater., 11 (1999), pp. 1307-1311
21. Q. Chen, W. Zhou, G.H. Du, L.-M. Peng, Trititanate Nanotubes Made via a Single Alkali Treatment, Adv. Mater., 14 (2002), pp. 1208-1211
22. J. Yu, H. Yu, Facile synthesis and characterization of novel nanocomposites of titanate nanotubes and rutile nanocrystals, Mater. Chem. Phys., 100 (2006), pp. 507-512
23. G. Armstrong, A.R. Armstrong, J. Canales, P.G. Bruce, TiO_2(B) Nanotubes as Negative Electrodes for Rechargeable Lithium Batteries, Electrochem. Solid-State Lett., 9 (2006), p. 139
24. C. Xu, Y. Zhan, K. Hong, G. Wang, Growth and mechanism of titania nanowires Solid State Commun., 126 (2003), pp. 545-549
25. H. Yu, J. Yu, B. Cheng, M. Zhou, Effects of hydrothermal post-treatment on microstructures and morphology of titanate nanoribbons, J. Solid State Chem., 179 (2006), pp. 349-354
26. L.-Q. Weng, S.-H. Song, S. Hodgson, A. Baker, Synthesis and characterisation of nanotubular titanates and titania, J. Eur. Ceram. Soc., 26 (2006), pp. 1405-1409
27. Z.Y. Yuan, J.F. Colomer J F, B.L. Su, Titanium oxide nanoribbons, Chem. Phys. Lett., 363 (2002), pp. 362-366

28. S.Y. Yuan, B.L. Su, Titanium oxide nanotubes, nanofibers and nanowires, Colloids Surf, A Physicochem Eng Asp., 241 (2004), pp. 173-183
29. A.F. Ghanem, A. El-Gendi, M.H. Abdel Rehim, K.M. El-Khatib, Hyperbranched polyester and its sodium titanate nanocomposites as proton exchange membranes for fuel cells, RSC Adv., 6 (2016), pp. 32245-32257
30. M. Sasani Ghamsari, A.R. Bahramian, High transparent sol–gel derived nanostructured TiO_2 thin film, Mater. Lett., 62 (2008), pp. 361-364
31. Prasanna, K.M. Usha, M.S. Hegde, Highly recyclable $Ti_{0.97}Ni_{0.03}O_{1.97}$ catalyst coated on cordierite monolith for efficient transformation of arylboronic acids to phenols and reduction of 4-nitrophenol, Dalton Trans., 50 (2021), pp. 14223-14234
32. K. Nagaveni, M.S. Hegde, N. Ravishankar, G.N. Subbanna, G. Madras, Synthesis and Structure of Nanocrystalline TiO_2 with Lower Band Gap Showing High Photocatalytic Activity, Langmuir, 20 (2004), pp. 2900-2907
33. M.F. Abdel Messih, M.A. Ahmed, A. Soltan, S.S. Anis, Facile approach for homogeneous dispersion of metallic silver nanoparticles on the surface of mesoporous titania for photocatalytic degradation of methylene blue and indigo carmine dyes, J. Photochem. Photobiol. A, 335 (2017), pp. 40-51
34. Z.M. Abou-Gamra, M.A. Ahmed, Synthesis of mesoporous TiO_2–curcumin nanoparticles for photocatalytic degradation of methylene blue dye, J. Photochem. Photobiol. B, 160 (2016), pp. 134-141
35. M.R.D Khaki, M.S. Shafeeyan, A.A. Abdul Raman, W.M.A. Wan Daud, Evaluating the efficiency of nano-sized Cu doped TiO_2/ZnO photocatalyst under visible light irradiation, J. Mol. Liq., 258 (2018), pp. 354-365
36. C.H. Nguyen, C.C. Fu, R.S. Juang, Degradation of methylene blue and methyl orange by palladium-doped TiO_2 photocatalysis for water reuse: Efficiency and degradation pathways, J. Clean. Prod., 202 (2018), pp. 413-427